SUPPLEMENTAL MATERIAL

Hoves et al., https://doi.org/10.1084/jem.20171440

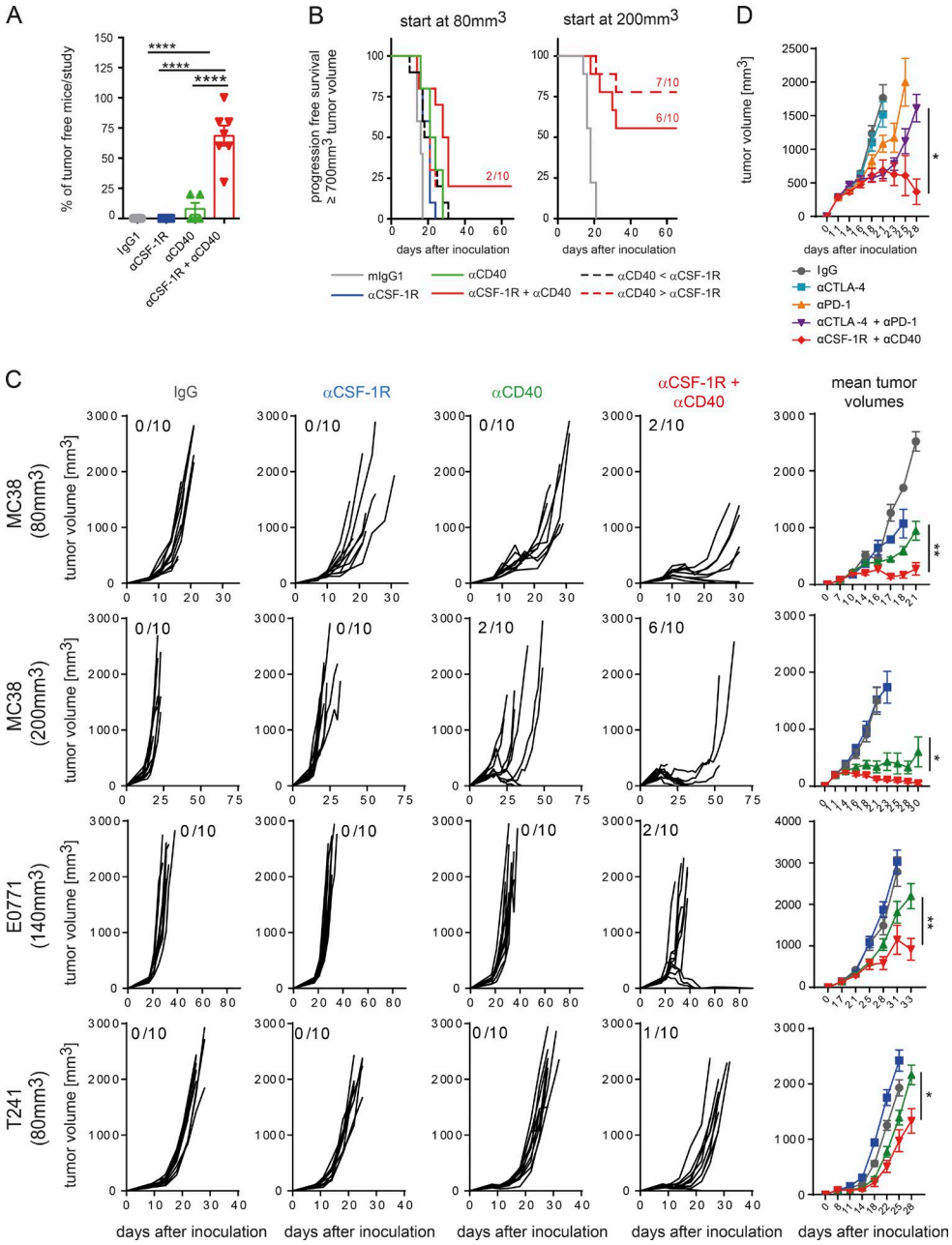

Figure S1. **Sequencing of αCSF-1R+αCD40 treatment and single tumor volumes of responsive tumor models. (A)** Number of animals that completely rejected tumors and that were ∼30 d tumor free pooled from all studies performed using MC38 at a starting tumor volume ≥100 mm^3 (studies n = 3 IgG 0/30, studies n = 3 αCSF-1R 0/30, studies n = 4 αCD40 4/40, and studies n = 7 αCSF-1R+αCD40 47/70; each data point represents numbers of tumor-free animals of n = 10 animals per experimental group). Data are depicted as means ± SD and were analyzed by one-way ANOVA and Tukey correction; asterisks indicate p-values with ****, $P < 0.0001$. **(B)** Sequencing of αCSF-1R+αCD40 influences tumor rejection rate in small but not in larger tumors. Mice were inoculated with MC38 tumors, and treatment was started at 80 or 200 mm^3, respectively. Treatment schedule was alternated in the αCSF-1R+αCD40 combination group by changing the application of αCD40 administration concomitant with αCSF-1R (αCSF-1R+αCD40), 2 d ahead of αCSF-1R (αCD40>αCSF-1R) or 2 d after αCSF-1R treatment (αCSF-1R>αCD40). Animals were graphically censored once the tumor volume reached ≥700 mm^3, and the numbers in graphs indicate numbers of tumor-free mice within the specific group (n = 10 for each group). **(C)** Matching single tumor volume graphs as well as mean tumor volumes per group to Fig. 1 (B and E) in MC38, E0771, and T241. Animals were sacrificed when termination criteria of the specific animal ethics approval were reached. Statistical analyses of mean tumor volumes were only performed for the last time point depicted by two-tailed Student's t test and comprising a minimum of seven animals per group. This criterion was not reached for IgG- or αCSF-1R–treated animals at this particular time point, and therefore these groups were excluded from statistical analyses. **(D)** Mean tumor volumes of the CTLA-4+PD-1 versus CSF-1R+CD40 comparison from Fig. 1 D.

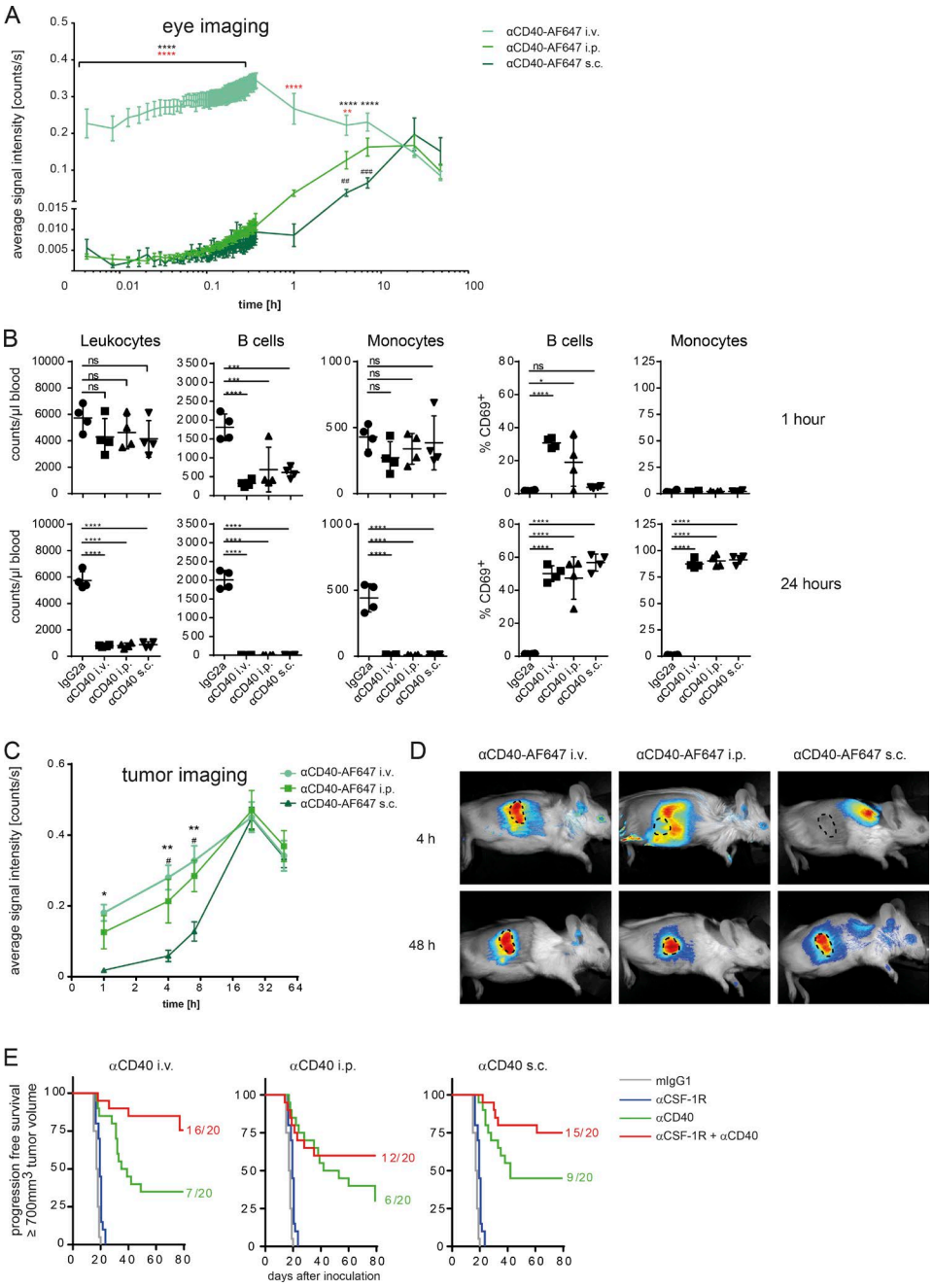

Figure S2. **The administration route of the αCD40 antibody has no influence on tumor rejection. (A, C, and D)** Female BALB/c mice were inoculated with CT26.WT tumors. Once tumor volumes reached 100 mm^3, αCD40-AF647 antibody was administered either i.v., i.p., or s.c. Fluorescent signal was monitored by eye imaging (A; Dobosz et al., 2014) or imaging of the tumor (C) as shown in D at the indicated time points. Dashed circles in D indicate tumors as superimposed from brightfield pictures. Statistical analysis was performed using two-way ANOVA and Tukey correction. Black asterisks indicate p-values of i.v. versus i.p.; red asterisks, of i.v. versus s.c; and hashmarks, of i.p. and s.c. administration. **(B)** Administration route influences immune cell distribution and CD69 expression at an early but not at a late time point in MC38 tumor–bearing mice. Total counts and expression of the early activation marker CD69 of total leukocytes, B cells, and monocytes were monitored 1 and 24 h upon administration of αCD40 antibody i.v., i.p., and s.c. in MC38 tumor–bearing C57BL/6 mice. Data are depicted as means ± SEM and analyzed using one-way ANOVA and Bonferroni correction. **(E)** The administration route of the αCD40 antibody does not impact on overall tumor rejection. Mice were inoculated with MC38 tumors and treated with either 30 mg/kg mIgG1 weekly, 30 mg/kg αCSF-1R weekly (i.p. only), 4 mg/kg αCD40, or a combination of both targeting antibodies in the large tumor setting. The αCD40 antibody was applied either i.v., i.p., or s.c. Animals were graphically censored once the tumor volume reached ≥700 mm^3, and the numbers in graphs indicate numbers of tumor-free mice within the specific group (n = 20 for each group). Data are pooled from two independent experiments. The same data of mIgG- and αCSF-1R–treated mice are shown in each graph for comparison. * and #, $P < 0.05$; ** and ##, $P < 0.01$; *** and ###, $P < 0.001$; ****, $P < 0.0001$. ns, not significant.

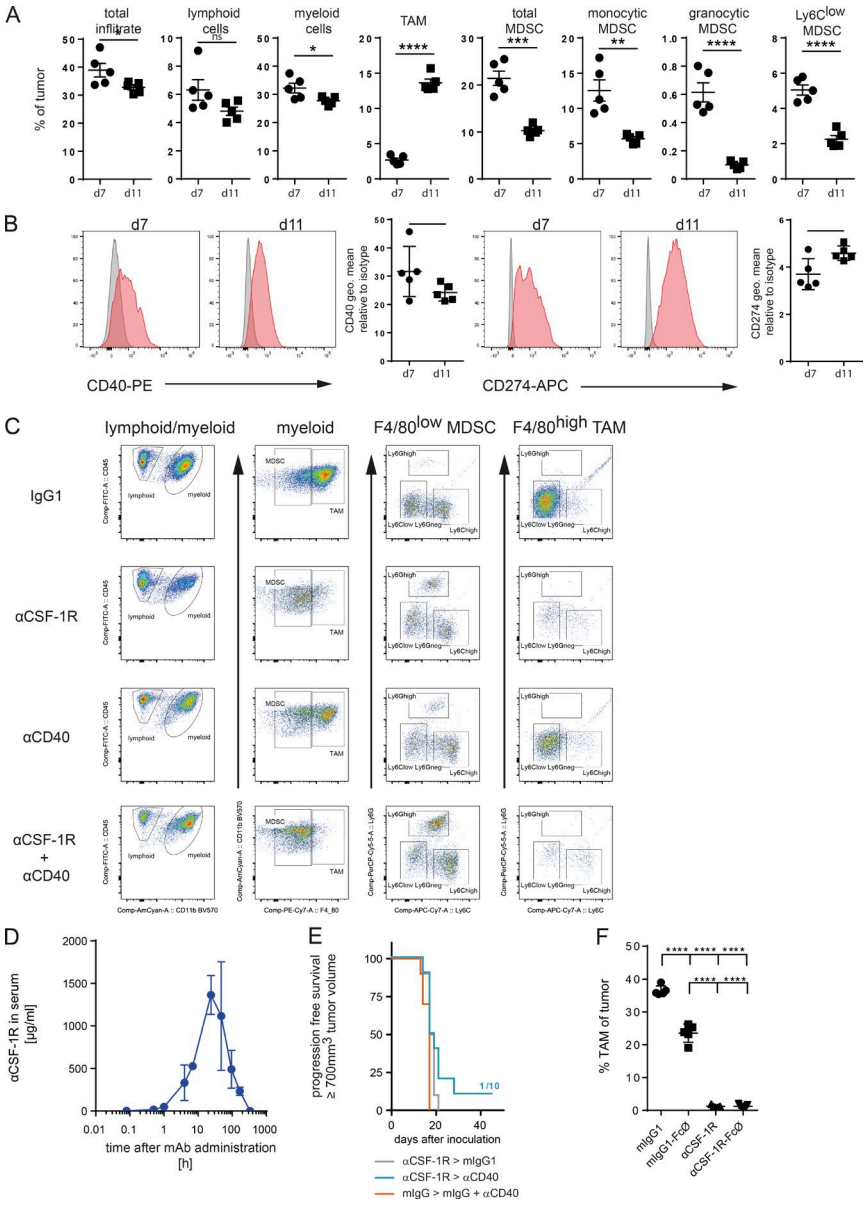

Figure S3. **Characteristics of the myeloid infiltrate of large versus small MC38 tumors and depletion of TAMs. (A and B)** The infiltrate of large MC38 tumors is dominated by TAMs, whereas smaller tumors are dominated by MDSC populations. MC38 tumors were inoculated and allowed to grow for 11 or 7 d, respectively. Tumors were analyzed by flow cytometry for the different myeloid subpopulations described. (B) Exemplary histograms for CD40 and CD274 expression from TAMs are shown in A. For directed comparison, geometric mean of CD40 and CD274 expression was normalized to the geometric mean of the matching isotype control on TAMs and is shown as relative values. Data in A and B are depicted as means ± SEM and analyzed using unpaired, two-tailed Student's *t* test for parametric data from $n = 5$ per group. One out of two independent experiments is shown. **(C)** Exemplary gating of myeloid cells within the tumor of animals corresponding to Fig. 2 A, treated with either 30 mg/kg mIgG1 weekly, 4 mg/kg αCD40 once, 30 mg/kg αCSF-1R weekly, or αCSF-1R+αCD40 combination. Tumors were analyzed on day 10 after having received two doses of αCSF-1R. **(D)** PK analysis of the αCSF-1R antibody from serum of MC38 tumor–bearing mice by ELISA using plate-bound murine CSF-1R and goat anti-mouse IgG1–specific antibody for detection. Time points analyzed were 5 and 30 min; 4 and 7 h; and 2, 4, 7, and 14 d upon i.p. injection of 30 mg/kg αCSF-1R clone 2G2 ($n = 3$). **(E)** Pretreatment with FcγR-competent IgG abolishes treatment effect of αCD40. MC38 tumor–bearing mice were pretreated on day 5 (50 mm^3) with either mIgG1 or αCSF-1R antibodies at 30 mg/kg. On day 11 (260 mm^3), the indicated antibodies were administered (30 mg/kg mIgG1 weekly or 4 mg/kg αCD40 once). Animals were graphically censored once the tumor volume reached ≥700 mm^3, and the numbers in graphs indicate numbers of tumor-free mice within the specific group ($n = 10$ for each group). **(F)** Depletion of TAMs by the G2G clone is independent of the Fcγ part of the antibody backbone. Scout animals of the TAM predepletion study in Fig. 2 D were analyzed for TAM content after two doses of 30 mg/kg of either mIgG1, mIgG1 incompetent in binding to FcγR (mIgG1-FcØ), or αCSF-1R clone 2G2 incompetent in binding to FcγR (αCSF-1R–FcØ; $n = 3$ per group). Data are depicted as means ± SD and analyzed using one-way ANOVA and Tukey correction; *, $P < 0.05$; **, $P < 0.01$; ***, $P < 0.001$; ****, $P < 0.0001$. ns, not significant.

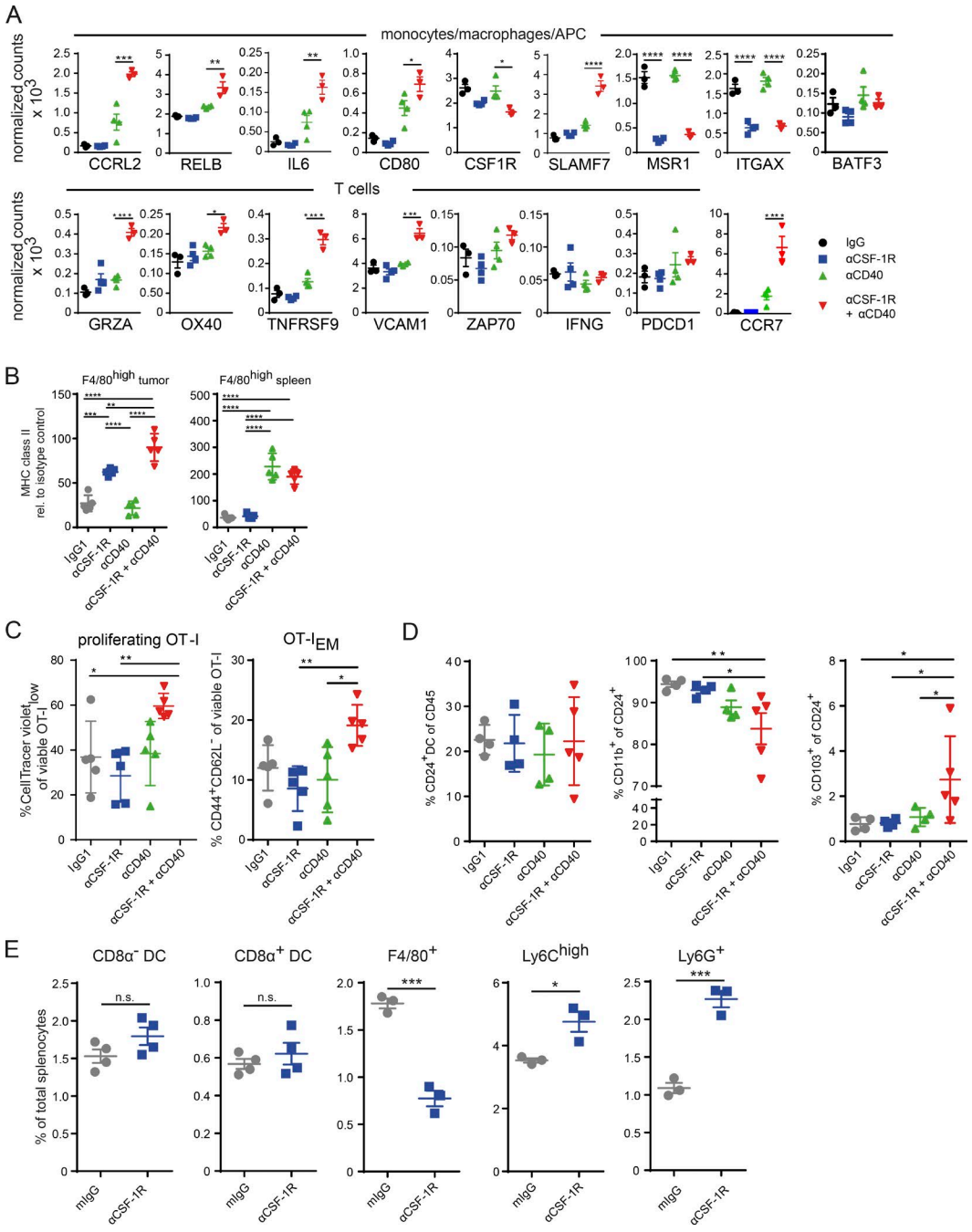

Figure S4. **Additional genes from NanoString and DC analysis. (A)** Additional genes form NanoString analysis for monocytes/macrophages/APCs and T cells. Data are depicted as means ± SEM and analyzed using one-way ANOVA and Tukey correction, and p-values are only shown for the comparison of αCD40 with αCSF-1R+αCD40. **(B)** MHC class II expression by F4/80^{high} macrophages in tumor and spleen of animals treated with 30 mg/kg mIgG1, 30 mg/kg αCSF-1R, 4 mg/kg αCD40, or a combination of both targeting antibodies for 3 d. Geometric mean of MHC class II is shown relative to the matching isotype control as individual values and means ± SD; statistical analysis by one-way ANOVA and Bonferroni correction. **(C)** αCSF-1R+αCD40 combination leads to enhanced OT-I priming. C57BL/6 mice were inoculated with MC38-OVA and received 10^7 CellTrace violet–labeled OT-1 T cells 1 d before the indicated treatment. On day 3, proliferation as well as effector memory T cell status was assessed from splenocytes upon start of treatment ($n = 5$ per group). Graphs show means ± SEM, statistical analysis by one-way ANOVA and Bonferroni correction. **(D)** Migratory CD103$^+$ DCs are elevated in αCSF-1R+αCD40 combination–treated MC38-OVA tumor. DCs were analyzed from tumors 16 h after administration of the indicated antibodies according to Broz et al. (2014). Graphs show means ± SEM, statistical analysis by Fisher's least significant difference test. **(E)** Spleens of MC38 tumor–bearing mice that were treated for 10 d with either mIgG or αCSF-1R, both 30 mg/kg, starting at 120 mm^3 tumor volume and were analyzed for myeloid cells as indicted by flow cytometry. Statistical analysis by two-tailed Student's *t* test with *, $P < 0.05$; **, $P < 0.01$; ***, $P < 0.001$; ****, $P < 0.0001$. n.s., not significant.

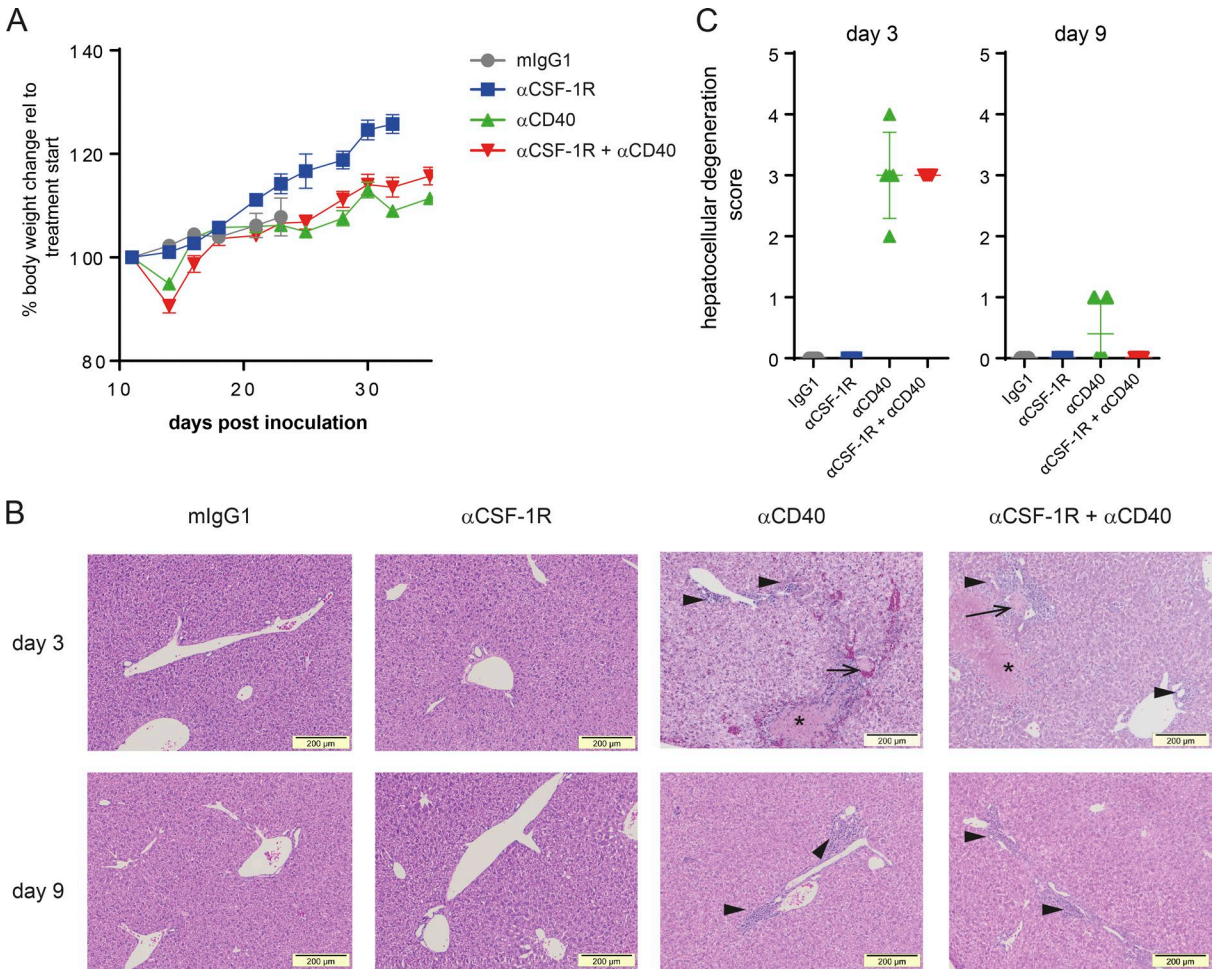

Figure S5. **αCSF-1R+αCD40 combination does not lead to additional signs of liver toxicity beyond αCD40 monotherapy. (A)** Bodyweight relative to the individual bodyweight at start of treatment. Animals were treated with either 30 mg/kg mIgG, 30 mg/kg αCSF-1R, 4 mg/kg αCD40, or the combination of both antibodies, and bodyweight was monitored at the indicated time points. *n* = 10 per group. **(B)** Liver H&E staining. Mice treated with αCD40 or with the combination of αCSF-1R+αCD40 showed on day 3 areas of hepatic necrosis (asterisks), thrombi (arrows), and infiltrates of mononuclear cells perivascular and in portal spaces (arrowheads). Minimal infiltrates of mononuclear cells were present perivascular and in portal spaces on day 9 after treatment. **(C)** Score of hepatocellular degeneration/necrosis on days 3 and 9 after start of treatment (*n* = 5 for all groups on day 3; *n* = 3 for mIgG and αCSF-1R on day 9; *n* = 5 for αCD40 and αCSF-1R+αCD40). Samples were scored by a board-certified veterinary pathologist (A.M. Giusti).

Supplemental tables are included in separate Excel and PDF files. Table S1 is a comparison of RNA sequencing with published signatures. Table S2 is a statistical analyses of tumor growth. Table S3 is a comparison of whole tumor NanoString and isolated TAM RNA sequencing expression data. Table S4 is a quantification of IHC stainings on patient tumor samples.

REFERENCES

Broz, M.L., M. Binnewies, B. Boldajipour, A.E. Nelson, J.L. Pollack, D.J. Erle, A. Barczak, M.D. Rosenblum, A. Daud, D.L. Barber, et al. 2014. Dissecting the tumor myeloid compartment reveals rare activating antigen-presenting cells critical for T cell immunity. *Cancer Cell.* 26:638–652. https://doi.org/10.1016/j.ccell.2014.09.007

Dobosz, M., S. Strobel, K.G. Stubenrauch, F. Osl, and W. Scheuer. 2014. Noninvasive measurement of pharmacokinetics by near-infrared fluorescence imaging in the eye of mice. *J. Biomed. Opt.* 19:016022. https://doi.org/10.1117/1.JBO.19.1.016022